IEEE Transactions on Nuclear Science, Vol. NS-28, No. 3, June 1981

ORBIT STUDIES FOR THE 100 MeV ALADDIN RACETRACK MICROTRON INJECTOR*

M.A. Green
UW Synchrotron Radiation Center
3725 Schneider Drive
Stoughton, WI 53589

Summary

This paper describes the computer simulation of electron motion in the 100 MeV racetrack microtron used as an injector on the SRC/Aladdin storage ring. Further details on these machines appear elsewhere in these proceedings.[1,2] These computations are for a single particle free to move in all three spacial dimensions. Programing utilizes idealized field models to simplify investigation of different machine configurations and to speed computations. First the program is used to assure that a central (having zero phase and transverse oscillation amplitudes) particle is properly accelerated. Then the motion of particles differing in initial phase and transverse coordinates is assured. The survival of particles under these varying conditions provides, then, information about the stability limits of the machine.

Introduction

Design of the Aladdin RTM (racetrack microtron) injector[2] was greatly influenced by careful parameter selection using computer simulation of the single particle motion. Despite the simplicity of the RTM such simulation makes possible studying the effect of very many variables on the motion of the beam. Programing was in FORTRAN and run interactively on a DEC VAX 11/780 computer. Design capability was measurably increased by the ability to immediately present chosen results in hardcopy graphic form.

The machine layout as dealt with here is shown schematically in Fig. 1. The constituent parts affecting the beam are the magnets and the drift space between them containing a linac. For reference, note the coordinate directions shown. Particle tracking begins at the entrance to the linac as the beam first enters from the injection line (not shown).

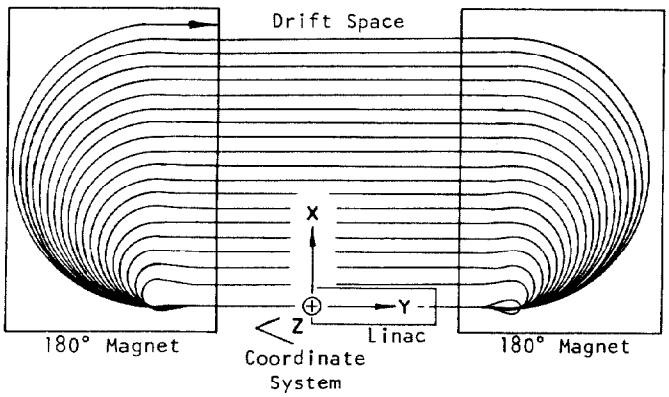

FIGURE 1 SCHEMATIC LAYOUT OF THE RTM AND OF THE ORBITAL COMPUTATIONS
Particle motion begins at (0,0,0) in the $+\hat{y}$ direction

The (computer simulation) program does have limitations which must be acknowledged. In part this stems from the initial conditions assumed, including:

- not including motion back through the injection transport line; and,
- the number, type, and ordering of machine components.

Also, the program does not exactly mirror reality, especially in that:

- collective beam effects are not treated; and,
- static magnetic and rf fields in the magnet and linac, respectively, are mostly idealized as are some of the equations dealing with them (e.g. at the linac apertures).

Computations

It is appropriate in these problems to write the equations of motion in dimensionless form.[3] In this formulation the familiar dimensional variables are re-expressed as follows:

Dimensional Variables	Dimensionless Variables
t, time	$\Phi = 2\pi ft$, total phase ϕ $(-\pi,+\pi)$, relative phase
X,Y,Z, spacial	$x = X/\lambda\!\!\!^{-}$, $y = Y/\lambda\!\!\!^{-}$, $z = Z/\lambda\!\!\!^{-}$
E, energy	$\gamma = E/m_0c^2$
$\vec{V}$, velocity	$\vec{\beta} = \vec{V}/c$: $\beta^2 = 1 - 1/\gamma^2$
$\vec{P}$, momentum	$\vec{p}(=\vec{\beta}\gamma) = \vec{P}/m_0c$: $p^2 = \gamma^2 - 1$
$\vec{B}$, magnetic fields	$\vec{\Omega} = \vec{B}/B_0$
$\vec{E}$, electric fields	$\vec{\varepsilon} = \vec{E}/B_0c$

where: f = rf frequency
c = light speed
$\lambda = c/f$; $\lambda\!\!\!^{-} = \lambda/2\pi$
m_0 = electron rest mass
q = electron charge
$B_0 = 2\pi fm_0/q$, the cyclotron magnetic field.

With these substitutions the equations of motion become (with "·" signifying differentiation wrt ϕ):

$$\dot{\vec{p}} = \vec{\varepsilon} + \vec{\beta}\times\vec{\Omega} \qquad (1)$$

where: $\vec{\varepsilon} = \vec{\varepsilon}(\vec{r},\phi)$ in the linac
$\vec{\Omega} = \vec{\Omega}_{dc} + \vec{\Omega}_{rf}$
$\vec{\Omega}_{dc} = \vec{\Omega}_{dc}(\vec{r})$ in the magnets only
$\vec{\Omega}_{rf} = \vec{\Omega}_{rf}(\vec{r},\phi)$ in the linac only.

Solution of Eq. 1 proceeds in each region of the machine: the magnets, the linac, and (trivially) the drift spaces. Except in the latter case, these equations are solved numerically with an 8x10 Runge Kutta routine.[4] As described below each region is appropriately subdivided into sections, each corresponding to a discrete field model. As the motion is calculated, continual checks are made in each section to verify that bounds in position, phase, momentum, etc. have not been exceeded.

Field Models and Equations

Magnets. In the computations, as in reality, the magnetic fields in the two magnets are identical but for the mirror symmetry (cf. Ref. 2). Neglecting a separate discussion of the localized perturbation on the last orbit for extraction, the measured median plane magnetic field for all other orbits and magnet cross sections is shown in Fig. 2. In the computations this magnetic field is approximated (to facilitate varying parameters and computing speed) by the piecewise continuous field model also shown in Fig. 2. In this case the fields on the rhs of Eq. 1 are:

0018-9499/81/0600-2428$00.75©1981 IEEE

$$\vec{\varepsilon},\ \vec{\Omega}_{rf} = 0;\ (\vec{\Omega}_{dc})_x = 0 \qquad (2)$$

Section	$(\vec{\Omega}_{dc})_z$ =	$(\vec{\Omega}_{dc})_y$ =
7	$R\Omega(y_a-y)/(y_b-y_a)$	$zR\Omega/(y_a-y_b)$
8	$-R\Omega$	0
9	$[-R+(1+R)/(y-y_c)/(y_d-y_c)]\Omega$	$z(1+R)\Omega/(y_d-y_c)$
10	$\Omega + G(y-y_d)$	zG

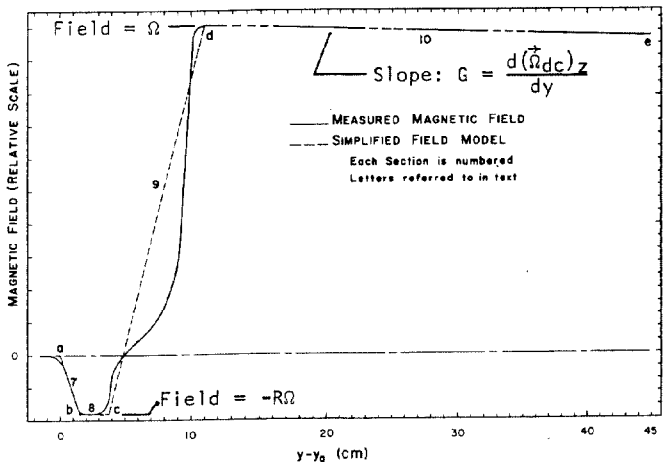

FIGURE 2. MEDIAN PLANE MAGNETIC FIELDS - MEASURED AND MODEL

In section 9 the difference between the actual and model fields can be appreciable in which case the linear approximation is replaced by a table of measured values for final calculations.

Linac. The treatment of the linac fields is similar but complicated by the presence of both electric and magnetic rf fields, noncircular flight apertures, and two cell geometries (full and half) to consider. It is necessary to begin with an analysis of the important axial ($\hat{y}$) electric accelerating field. Its actual value was nearly approximated before construction with the LALA program[5] and measured after with a beadpull measurement. The axial field profile and the equivalent trapezoidal model for a full cell are shown in Fig. 3 (the case for a half cell is similar but involves an asymmetric profile). It is assumed that the noncircular apertures affect only the sloping field sections (1 and 3) and not the central section (2). Under these conditions, to first order in transverse (x and z) displacements for the linac axis:

Electric Fields[6]	Section 1	2	3
ε_x =	$-x\tilde{\alpha}S\cos\phi$	0	$+x\tilde{\alpha}S\cos\phi$
ε_y =	$S(y-y_g)\cos\phi$	$\varepsilon\cos\phi$	$\varepsilon - S(y-y_i)\cos\phi$
ε_z =	$-z\alpha S\cos\phi$	0	$+z\alpha S\cos\phi$

Magnetic Fields[7]	Section 1	2	3
$(\vec{\Omega}_{rf})_x$ =	$z\alpha S(y-y_g)\sin\phi$	$+\frac{1}{2}z\varepsilon\sin\phi$	$-z\alpha S(y-y_i)\sin\phi$
$(\vec{\Omega}_{rf})_y$ =	0	0	0
$(\vec{\Omega}_{rf})_z$ =	$-x\tilde{\alpha}S(y-y_g)\sin\phi$	$-\frac{1}{2}x\varepsilon\sin\phi$	$+x\tilde{\alpha}S(y-y_i)\sin\phi$

where: $S = \left|d(\varepsilon_y)/dy\right|_{\phi=0}$ is the slope of the field

and $\alpha = 1/(1+A)$; $\tilde{\alpha} = A/(1+A) \rightarrow \alpha + \tilde{\alpha} = 1$

with A = aperture height (z) to width (x) ratio.

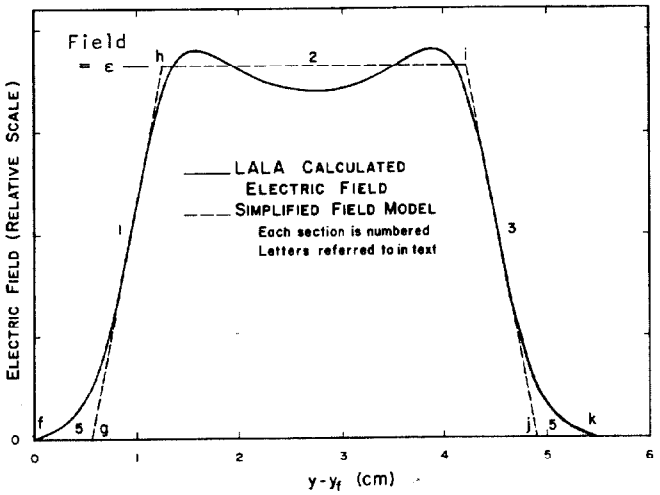

FIGURE 3. FULL CELL AXIAL RF ELECTRIC FIELDS - CALCULATED AND MODEL

One final note should be added as to the relative excitation between cells. The nominal phase shift between adjacent cells is π radians. However, moving outward in both directions from the center (feed) cell, additional small phase shifts[8] depending on intercell coupling and cell Q value have been accounted for in the program. Also, the field amplitudes of the several cells can be adjusted in accordance with either analytical or measured values.

Drift Spaces. Where drift spaces occur there is assumed to be zero field and the motion is simply transformed across them. These spaces exist between the major elements, the linac and magnets, and within the linac (sections 5 in Fig. 3).

Methods

In all there are 7 particle coordinates, 25 machine parameters, numerical integration values, and numerous particle bound limits that must be rationally established. In abbreviated form the process to fix these parameters is as follows.

Fix:

- Nominal energy gain per turn = 5 MeV
- Final kinetic energy approx. 100 MeV
- Linac geometry: f = 2800 MHz; 6 cells; π mode; standing wave; relative cell field amplitudes and phasing; nominal aperture diameter = 1 cm; all apertures with some aspect ratio.

Adjust:

- Overall linac excitation so that a 50 MeV (half full energy) electron passing through at the desired stable phase angle of 20° will gain 5 MeV.
- Main magnet field according to calculation[9]
- Reverse magnetic field length and strength to produce a colinear bend in the end magnet assembly for the central particle
- Drift spaces on either side of linac to reduce long term phase oscillation amplitude of the central particle arbitrarily close to zero
- Linac aperture aspect ratio to determine stability limits for radial motion; pick value which produces best vertical motion behavior about the central particle
- Vertical focusing characteristics: at low energy with the reverse magnetic field geometry; at high energy by varying the main magnetic field gradient.

Integration parameters having to do with step size and boundary proximity are reduced in magnitude so that the full energy beam motion remains unchanged.

Results

Based on Simulation

Once the machine parameters have been "tuned up" by the above procedure particles with varying initial conditions can be studied. One finds that phase-energy oscillation limits are imposed as by the theory of phase stability in these machines.[10] Radial oscillation amplitude is limited by the radial width (.88 cm) of the linac flight apertures. And the vertical amplitude is limited by the vertical aperture (.66 cm) in the main magnetic field poles. Examples of stable radial and vertical motion are shown in Figs. 4 and 5, respectively. Transformed back to injection some of these stability limits are as follows.

Table. Some Machine Stability Limits at Injection

Given: The Initial "Central" Particle Coordinates

Phase	ϕ_o	1.233 rad
Kinetic Energy	KE_o	50 keV
Transverse Coords.	x_o, $(p_x)_o$, z_o, $(p_z)_o$	0

Find: These Coordinate Axes Intercepts with the Motionally Stable Volume

Phase	$.17 \leq \phi_o \leq 1.62$ radians
Kinetic Energy	$27 \leq KE_o \leq 71$ keV
Radial - Position	$\lvert x_o \rvert \leq .090$ or $\lvert X_o \rvert \leq .15$ cm
Divergence	$\lvert (\alpha_x)_o \rvert \leq .046$ radians
Vertical - Position	$\lvert z_o \rvert \leq .18$ or $\lvert Z_o \rvert \leq .31$ cm
Divergence	$\lvert (\alpha_z)_o \rvert \leq .052$ radians

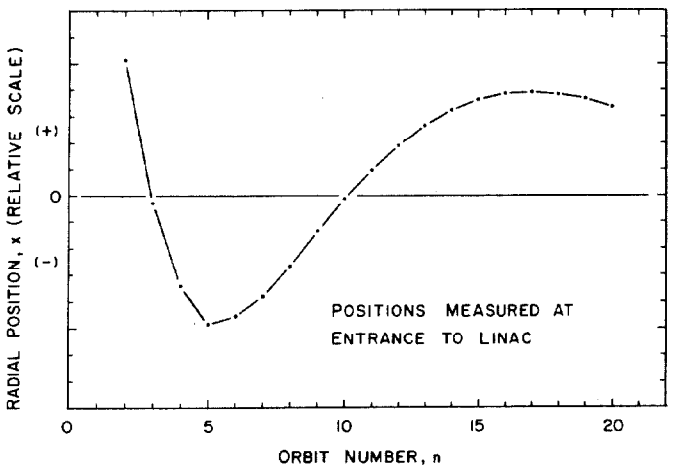

FIGURE 4. EXAMPLE OF STABLE RADIAL MOTION

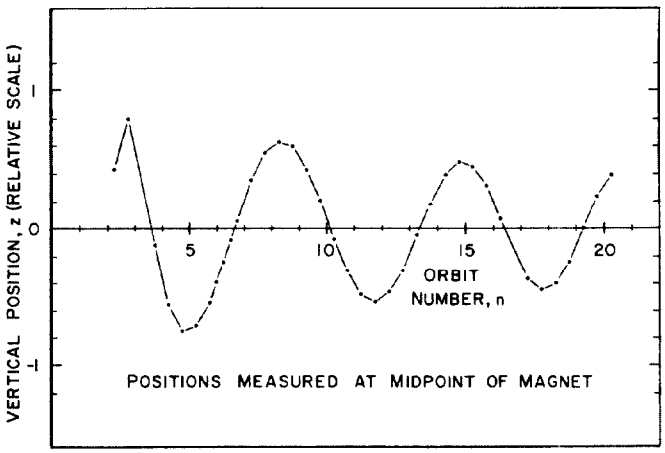

FIGURE 5. EXAMPLE OF STABLE VERTICAL MOTION

Compared with Operation

Originally this paper was to be completed with a comparison of the numerical design and actual operation of the machine. Regrettably, the RTM injector is not as yet operational and these results will have to be reported at a later time.

Acknowledgments

The author would like to thank Dr. Servranckx for providing the Runge Kutta code mentioned in the text. Also gratefully appreciated are the helpful discussions with Walt Trzeciak and the computing staff, both from our laboratory, in developing the computer programs.

References

1. E.M. Rowe, et al., *Status of the Aladdin Project*, these proceedings.

2. M.A. Green, et al., *Design and Operation of the 100 MeV Aladdin Microtron Injector*, these proceedings.

3. See, e.g.: S.P. Kapitza, et al., Soviet Physics, JETP 14, 266 (1962); see especially p. 272.

4. R. Servranckx, Particle Accelerators 6, 83 (1975).

5. W.F. Rich and M.D.J. MacRoberts, LASL Report LA-4219 (1969).

6. For transverse fringing components see: S.P. Kapitza and V.N. Melekhin, *The Microtron* Harwood Academic Publishers, LTD.; London (1978); Chap. 4, Secs. 1-4.

7. By approximate solution of Maxwell's Eqs. given the electric fields above.

8. See, e.g.: T.I. Smith, HEPL Report 437 (1966); Sec. II-C.

9. As by appropriate use of Eq. 1 in Ref. 2 above.

10. C. Henderson, et al., Proc. Phys. Soc. London B, 66-1, 41 (1953).

*Work performed under NSF contract DMR-7708657.